Published in final edited form as:
J Neurosci Res. 2009 May 15; 87(7): 1718–1727. doi:10.1002/jnr.21973.

Vessel Microport Technique for Applications in Cerebrovascular Research

Lei Chen[1,2], **Karin R. Swartz**[2], and **Michal Toborek**[1,2,★]

[1]Molecular Neuroscience and Vascular Biology Laboratory, Lexington, Kentucky

[2]Department of Neurosurgery, University of Kentucky Medical Center, Lexington, Kentucky

Abstract

Cerebrovascular research suffers from a lack of reliable methods with which to deliver exogenous substances effectively into the central nervous system (CNS) of small experimental animals. Here we describe a novel vessel microport surgical technique for a variety of cerebrovascular applications that is reproducible and well tolerated in mice. The procedure is based on the insertion of a vessel microport into the external carotid artery for substance delivery into the CNS via the internal carotid artery. The method results in selective substance delivery into the ipsilateral hemisphere. Other novel aspects of this surgical technique include the ability to perform multiple injections, study of conscious mice well removed from surgery, and lack of occlusion of the common or internal carotid artery that allows carotid flow to be maintained. The feasibility of this technique has been validated by infusion of HIV Tat protein to induce permeability of the blood–brain barrier and by implantation of tumor cells to establish a brain metastasis model. Thus, the described vessel microport technique can be employed in a variety of cerebrovascular research applications.

Keywords

CNS drug delivery; vessel port; mouse carotid artery surgery; HIV Tat protein; brain metastasis

Substance delivery into the brain has been the main obstacle in cerebrovascular research and clinical practice (Begley, 2004; Muller et al., 2006; Reddy et al., 2006; Witt and Davis, 2006; de Boer and Gaillard, 2007; Pardridge, 2007). Part of these difficulties is due to the existence of the blood–brain barrier (BBB), which is formed of cerebral microvascular endothelial cells with the support and regulatory role of the surrounding astrocytes, pericytes, and neurons (Abbott et al., 2006; Kim et al., 2006).

Several strategies have been developed to facilitate substance delivery to targeted areas in the CNS (Bickel et al., 2001; Misra et al., 2003; de Boer and Gaillard, 2007; Kumar et al., 2007). For example, exogenous substances can be administered into the nasal or ophthalmic organs. The substance can then enter the CNS through the olfac-tory or ophthalmic nerves in an axoplasmic transport manner. However, a low applicable dosage and slowness in the delivery limit its application (Thorne et al., 1995; Vyas et al., 2005). Other forms of local administration are intra-sheath, intracerebral, or intraventricular injections or implants (Frisella et al.,2001; Wei et al., 2001;Wu et al., 2006; Pignataro et al., 2007). Although these methods allow

★Correspondence to: Michal Toborek, MD, PhD, Molecular Neuro-science and Vascular Biology Laboratory, Department of Neurosurgery, University of Kentucky Medical Center, 593 Wethington Bldg., 900 S. Limestone, Lexington, KY 40536. E-mail: E-mail: michal.toborek@uky.edu.

substance delivery into the surgically targeted structures, these approaches are traumatic to the CNS, and the administered volume is limited to small amounts. In addition, they are associated with a quick removal by the cerebrospinal fluid (CSF) and/or low penetration range to the brain parenchyma (Sugiyama et al., 1999; Pardridge, 2002).

Because of the limitations of local substance delivery, a systemic delivery remains the most popular means of administration of exogenous substances into the brain. The most commonly used are the oral-intestine, pulmonary, subcutaneous, and intravenous routes. In laboratory mice, oral administration or i.v. injections through the tail veins are commonly used. However, the oral intake or tail vein injections are subjected to the first-pass effect through the liver and clearance by the lungs, which can deactivate or diminish drug activity (Bardelmeijer et al., 2002; Sebestyen et al., 2006; Oh et al., 2007). Furthermore, a systemic administration results in distribution throughout the body and uptake by other organs before they can reach the brain microcirculation (Vantyghem et al., 2003; Huang et al., 2007). These reasons necessitate a larger dosage of administered substances that can increase the risk of the development of side effects and toxicity (Liu et al., 2005; Kumar et al., 2007).

Taking into consideration the uniqueness of the CNS circulation, the ideal method of substance delivery into the brain should 1) be associated with minimal trauma, 2) preserve the integrity of the neuronal network, 3) allow for repeated administrations, and 4) allow achieving high substance concentrations in the brain. We have developed a novel surgical technique, based on these criteria, to deliver exogenous substances into the brain via a vessel microport inserted into the external carotid artery (ECA) that allows repeated substance delivery into the ipsilateral brain hemisphere via the internal carotid artery (ICA).

MATERIALS AND METHODS

Surgical Procedures

To construct the vessel microport, a 3-cm Micro-Renathane Implantation Tubing (MRE010, part 9049−13−00; Braintree Scientific, Braintree, MA) was connected and glued (Super Glue; Fisher Scientific, Pittsburgh, PA) to a commercially available Microport (0.54 mm diameter; DaVinci Biomedical Research Products, South Lancaster, MA). Then, the port was filled with 50 μl heparinized saline (10 IU/ml) and gas sterilized before the surgery.

C57Bl/6 mice (25−32 g; Charles River Laboratories, Wilmington, MA) were maintained under environmentally controlled conditions and subjected to a 12-hr light/dark cycle, with food and water provided ad libitum. The animals were acclimatized to the facility for 7 days prior to the start of the experiments. All procedures and handling techniques were in strict accordance with the National Institutes of Health guidelines for the care and use of laboratory animals and approved by the Institutional Animal Care and Use Committee.

The main elements of the surgical procedure are illustrated in Figure 1. The mice were anesthetized with isoflurane in oxygen. Ventrally, both sides of the neck were shaved. The entire area was then scrubbed with betadine three times, alternating with 70% alcohol. All instruments were sterilized prior to surgery. The procedure was performed with surgical masks, gowns, and sterile gloves over scrubbed hands.

A midline neck incision was made under the operating microscope, followed by isolation of the common carotid artery (CCA), ECA, and ICA. We routinely operated on the left carotid artery. To isolate the ECA, the cranial thyroid artery was identified, ligated, and cut distal from the ligated point. In addition, the occipital artery was ligated and cut to avoid substance delivery into the occipital region. Silk sutures around the vessel stumps were tied tightly to prevent bleeding. The ECA was then ligated with 6−0 silk suture distal from the ICA. Flow through

the CCA and the ICA was temporarily restricted by placing a vessel clip (Fine Science Tools, Foster City, CA) on each of these arteries. A small incision was then made on the ECA, and the tubing tip was inserted through the incision and advanced back toward the CCA until it reached the bifurcation point. The tubing was secured with two knots around the ECA and an additional knot around a muscle. Then, the vessel clips on the CCA and the ICA were removed. The distal part of the tubing was tunneled under the skin to the dorsal region of the neck, and the microport was buried under the skin. The wound on the ventral region of the neck was closed, and clotting in the tubing was prevented by flushing the microport with 50 ll heparinized saline (10 IU/ml) every day during the first week postsurgery and then every other day. The mice were allowed to recover after surgery for 1 week. The microports were maintained for up to 30 days.

To monitor cerebral blood flow during the surgical procedure, a laser Doppler probe was glued to the skull in the area corresponding to the brain region that receives the blood from the ipsilateral middle cerebral artery (MCA); flow was recorded by using a PeriFlux System 5000 Laser Doppler unit (Perimed, North Royalton, OH).

Injections Through the Vessel Port

Mice were anesthetized with isoflurane in oxygen, and the injections were made through the skin to the vessel port with a 27-G needle. The port was flushed with 30 μl saline, followed by the substance or cell delivery in a volume that did not exceed 200 μl. After the injection, the port was flushed again with 30 μl heparinized saline to prevent blood clotting in the tubing.

We compared the influence of substance delivery via the vessel port vs. an intracranial injection on the integrity of the neuronal and microvessel networks. To perform intracranial injections, a 1-mm burr hole was made at 1.8 mm lateral and 1.7 mm caudal to bregma. A 30-G needle attached to a 2-μl Hamilton syringe was then stereotactically inserted into the cortex at a depth of 2.1 mm from the dura. Evan's blue solution (1% in PBS; 2 μl) was injected over 2 min with a stereotaxic injector. The needle was left in place for 1 min and then slowly withdrawn to minimize tissue damage. On the following day, the brains were removed and fixed, and 20-μm sections were prepared. The slices were stained with cresyl violet for neurons.

To visualize the microvascular network, mice were injected via vessel port and intracranially as described above and then perfused with heparinized saline, followed by per-fusion with 4 ml 2 mg/ml fluorescein isothiocyanate (FITC)-albumin solution (Sigma, St. Louis, MO). The brains were sliced and the images were taken with a fluorescent microscope (excitation 485 nm, emission 535 nm).

Selectivity of Substance Distribution Through the Vessel Port

To verify that injections via the vessel port resulted in substance distribution consistent with the area supplied by the ICA, carbon black (1% solution in 20% gelatin; Sigma) was injected via the installed port into the anesthetized mice. Gelatin solution was prepared in phosphate-buffered saline (PBS). After injection, brains were harvested and photographed to document the affected vessel network.

In the next series of experiments, 200 μl 2 M mannitol (Sigma) in PBS was administered through the vessel microport, followed by injection of 200 μl 2% Evan's blue in PBS through the tail vein. Evan's blue readily combines with the circulatory albumin; therefore, the presence of blue staining in the brain parenchyma indicates Evan's blue-labeled albumin penetration across the BBB. Mice were perfused with heparinized saline 15 min after the Evan's blue injection. The brains were harvested, and 100-μm cryostat sections were prepared, analyzed, and photographed.

Assessment of the BBB Integrity

Mice (five animals per group) received injections with 25 lg HIV Tat protein in PBS through the vessel port, i.p., or tail vein. Control group of mice received 200 μl PBS (negative control) or 2 M mannitol in PBS (positive control) via the installed vessel port. After a 24-hr exposure to Tat, 200 μl sodium fluorescein (Sigma) in PBS (6 mg/ml) was injected through the tail vein and allowed to circulate for 15 min. Then, mice were anesthetized with isoflurane in oxygen and perfused with 30 ml heparinized saline through the left ventricle. The brains were harvested, the contralateral hemispheres were discarded, and the ipsilateral hemispheres were homogenized in PBS (1:10 g/v). The homogenates were precipitated in 15% trichloroacetic acid (1:1 v/v) and centrifuged at 1,000*g* for 10 min. The pH was adjusted by adding 125 μl 5 M NaOH to 500-μl supernatant aliquots, and fluorescence was detected with a fluorescence plate reader with excitation at 485 nm and emission at 530 nm.

Injection of Tumor Cells Into the Brain Hemisphere

To determine the feasibility of the vessel port injection to induce brain metastasis formation, 1 million luciferase-labeled D122 (D122-Luc) lung cancer cells in 100 μl PBS were administered through the port into the left hemisphere. Control mice received injections of 200 μl PBS. The growth of tumor cells was monitored every week for 4 weeks by i.p. injections of 2 mg luciferin in 100 μl PBS and determination of bioluminescent signals using the IVIS imaging system (Caliper Life Sciences, Hopkinton, MA). The measurements were performed through the skulls of live and anesthetized mice. After the mice were sacrificed, bioluminescent intensity was also determined in isolated brains. Tumor growth was determined as the number of emitted photons/sec/cm^2.

RESULTS

Surgery and Brain Analysis for Tissue Integrity

All mice survived the procedure, and the vast majority of them recovered well from the surgery, with the body weight returning to normal values 2 days postoperation. Inflammation around the wound developed in only one mouse among 27 animals that received surgery. No other complications occurred during or after surgery.

Cerebral microcirculation was monitored during the carotid artery surgery by using the laser Doppler technique. As expected, cerebral flow decreased when the CCA was clipped (Fig. 2). However, the flow recovered instantly after clip release. In addition, infusion through the vessel port temporarily increased cerebral blood flow, indicating passing of the injected volume through cerebral microcirculation.

The installation and substance delivery via the vessel microport fully preserved the structural integrity of the brain. Figure 3 compares the brains from mice with installed vessel port with mice that received intracranial injection. Although the brains from mice that received injections via the vessel port are intact, the intracranial needle insertion resulted in substantial tissue damage along the needle mark (arrows in Fig. 3B,D,F). Other typical complications resulting from intracranial injections are hemorrhagic cortex damage (Fig. 3D,F, arrows) and disrupted cortex structures as indicated by cresyl violet staining (Fig. 3F, arrow). Evan's blue (2 μl) administered intracranially spreads locally around the injection site (Fig. 3B). This fact illustrates that substance delivery via direct intracranial injections has very limited distribution.

We also evaluated the integrity of microvessels in mice with installed vessel port compared with mice that received intracranial injections (Fig. 4). Vessel port delivery fully preserved the microvessel network as determined by staining for FITC-albumin. In contrast, micro-vessels

along and surrounding the needle puncture were disrupted and leaking as evidenced by FITC-albumin staining in brain parenchyma around the injection route.

Selectivity of Substance Delivery Via Vessel Microport

Injection of 1% carbon black in 20% gelatin was used to visualize the vascular network involved in substance delivery following injection via vessel microport. As indicated in Figure 5, the majority of administered carbon black distributed to the left (i.e., ipsilateral) hemisphere. In addition, carbon black was visualized in selected small cortical vessels (arrow) and within the olfactory bulb and cerebellum on the contralateral side.

In the next series of experiments, mice received the hyperosmotic solution of mannitol via the vessel port to open the BBB, followed by Evan's blue injection via i.p. injection. Figure 6 shows that Evan's blue penetrated into brain parenchyma with a pattern similar if not identical to that of carbon black, further confirming that the vessel port delivery results in substance distribution that affects primarily the ipsilateral hemisphere.

Application of the Vessel Microport To Evaluate HIV-1-Related Disruption of the BBB

Evidence indicates that HIV-1 can enter the brain early in infection. In addition, disruption of the BBB in the course of HIV-1 infection has been observed and confirmed in a variety of pathological studies (Rhodes and Ward, 1991; Krebs et al., 2000) and CSF studies (Singer et al., 1994) and by dynamic magnetic resonance imaging (Avison et al., 2002). One of the main factors that may be responsible for HIV-mediated disruption of the BBB is Tat protein that is released from HIV-1-infected cells. Therefore, we validated the vessel microport technique to assess whether Tat delivery can disrupt the BBB in mice. The integrity of the BBB was assessed by permeability of low-molecular-weight sodium fluorescein in the ipsilateral hemisphere. As indicated in Figure 7, injection with the same amount of Tat protein (25 μg) resulted in disruption of the BBB only when administered through the vessel port. In contrast, Tat delivery via tail vein or i.p. injections did not alter the integrity of the BBB. An injection with hyperosmotic mannitol was used as a positive control in these experiments.

Delivery of Tumor Cells Via Vessel Microport as the Model of Brain Metastasis Formation

The main route of metastatic formation in the brain is hematogenous spread across the BBB (Puduvalli, 2001; Patchell, 2003). Therefore, the installed vessel port was also used to deliver tumor cells into the mouse hemisphere as the model of development of brain metastasis. Injection of D122-Luc cells through the vessel port resulted in preferential localization of tumor cells to the ipsilateral brain hemisphere (Fig. 8). The imaging performed on living mice detected no bioluminescence signal 1 week postinjection of 1 million D122-Luc cells. However, mice that were imaged 2 weeks posttumor cell injection displayed marked bioluminescence on the ipsilateral site. Consecutive measurements at weeks 3 and 4 revealed a steady increase in intensity of the bioluminescent signals, indicating a growth of metastatic tumors (Fig. 8A,B). Imaging of isolated brains (Fig. 8C) at the end of the experiment demonstrated that tumor cells were visually evident in the ipsilateral hemisphere.

As indicated in Figure 8A, bioluminescent signals were also detected in the area corresponding to the nasal area of mice that received injection with D122-Luc cells. This signal was visible from week 3 onward; however, it was approximately 20 times less intense than the signal corresponding to metastatic growth in the cortex. Tumor development within the nasal area is consistent with blood supply via the branches originating from the CCA. The whole mouse imaging did not reveal bioluminescence signals outside the head, indicating highly specific tumor cell delivery and metastatic growth.

DISCUSSION

A major obstacle in substance delivery into the CNS is the BBB, which restricts the brain entry of substances that are water soluble or larger than 120 Da (Neuwelt, 2004). Therefore, several experimental methods have been developed to facilitate substance delivery across the BBB. Examples include high-dose intravenous chemotherapy, intraarterial drug delivery, local drug delivery via implanted polymers or catheters, BBB disruption, and biochemical modulation of drugs (Blakeley, 2008). The most common clinical approach to substance delivery into the CNS is to open the BBB by an injection of hyperosmotic mannitol, followed by specific drug. Such a protocol has been frequently used in treatment of primary CNS lymphoma (Muldoon et al., 2007). Therefore, our goal was to develop a surgical technique that targets small experimental rodents and allows multiple i.v. injections into the brain vasculature. Installation of the vessel port on the ECA proved to be highly suitable for multiple injections. To mimic the clinical setting of drug delivery, we first injected mannitol to open the BBB, followed by delivery of Evan's blue solution to stain the affected tissue. This procedure confirmed that the vessel port technique allows the delivery of exogenous substances to the ipsilateral hemisphere with high selectivity. It is also important that, after the microport injection, the substance can reach the brain at high concentration without being taken up via other microvascular circuits.

Another significant advantage of the surgical technique reported here is a minimal interference with the cerebral blood supply. Although three arteries (the ECA, cranial thyroid artery, and occipital artery) are ligated during the procedure, the blood supply can be restored from the neighboring vessels via crossing branches. Thus, the functionality of the blood supply to the head appears to be fully retained. Indeed, the mice showed normal behavior from the second day after the surgery and did not develop any adverse symptoms during the observation period for up to 30 days. In addition, monitoring of blood flow by laser Doppler technique indicated only a short (<10 min) decrease in blood flow during the period when the CCA was clipped for tubing insertion. Normal flow was then spontaneously restored, indicating that substances can be delivered to the cortex through the normal vascular route without the development of complications, such as cerebral hypoperfusion or ischemia.

Several justifiable concerns, such as duration of surgery, development of local inflammation, body response to foreign body, and/or blood clotting in the tubing, could be associated with the procedure. From our experience, a trained operator can install a vessel microport in approximately 1.5−2 hr; however, a highly skilled individual requires ~1 hr to complete the procedure. The blood clotting in the tubing is prevented by prefilling the port with heparinized saline before the surgery. Then, the vessel port requires a daily maintenance that includes flushing with 50 μl heparinized saline with a 27-G needle. The development of local inflammation can be mostly eliminated by using standard operating procedures, such as sterilized surgical instruments, wound cleaning, and operation under aseptic conditions. Although the mice tend to scratch the scar in the recovery process, only one mouse among 27 nipped the wound closure material and developed infection. The microport weighs only 0.6 g and is well tolerated by mice.

We tested the vessel port installation in the applications that model the disruption and/or involvement of the BBB in the course of HIV-1 infection and the formation of brain metastases. The inability of HIV to infect rodent cells is the main reason why there is no fully suitable or widely acceptable small-animal model of HIV-induced CNS disease. A frequently used model of HIVE is based on severe combined immune deficiency (SCID) mice that receive direct brain injection of human HIV-infected monocyte-derived macrophages (Persidsky et al., 2005). Although these animals develop encephalitis accompanying the BBB injury, it is based on injection of human cells into mouse brains, and stab wounds to the brain (as demonstrated in Fig. 3) can be difficult to quantify, particularly with respect to the BBB integrity. Therefore,

we employed injections of HIV protein Tat into the ICA as a model of HIV-related BBB injury. Evidence indicates that treatment with Tat can mimic all major vascular effects of HIV. In particular, exposure to Tat decreases the endothelial barrier function (Toschi et al., 2001; Avraham et al., 2004; Pu et al., 2005), stimulates transendothelial migration of monocytes (El-Hage et al., 2006), induces tight junction disruption (Andras et al., 2003; Pu et al., 2005), and up-regulates the efflux transporters (Hayashi et al., 2005, 2006).

The main advantage of using the vessel port is to administer Tat directly into the brain vasculature. Several reasons favor this method of Tat administration. For example, HIV-1 infection of the CNS is often characterized by widespread BBB injury; thus, injections into the anatomically defined brain structures (e.g., hippocampus or cortex) do not appear appropriate. In the course of HIV-1, brain capillaries are exposed to Tat from the luminal site, and such an exposure can be mimicked by injections into the ICA. Finally, injections of Tat into the ICA shorten the time required for Tat to reach the cerebral vasculature; therefore, Tat is less prone to be degraded in the blood stream. Indeed, injection of Tat via vessel port resulted in increased sensitivity of the BBB to Tat-induced toxicity, as we demonstrated in studies of the BBB integrity (Fig. 7).

Formation of brain metastases was another application in which the feasibility of the vessel port was evaluated. The brain is the major site of cancer metastases, and approximately 30 −40% of cancer patients develop primary or secondary brain metastases. It is estimated that ~200,000 new cases of brain metastases are diagnosed yearly in the United States (Subramanian et al., 2002). The most common sources of brain metastases are lung cancer (48% of all cases of brain metastases), breast cancer (22−25%; Subramanian et al., 2002), and melanoma (~15%). Therefore, we selected lung tumor cells (namely, D122-Luc cells) for use in the present study. In addition, these cells are of mouse origin, so they can be used for metastasis studies in immunocompetent mice (Margalit et al., 2003).

The brain presents a highly unique environment for metastatic growth that is fully met by the delivery of the tumor cells via vessel port installed in the ECA. For example, the brain lacks lymphatic drainage; however, it is highly vascularized. Therefore, the main route of metastatic formation into the brain is hematogenous spread across the BBB (Puduvalli, 2001; Patchell, 2003). Most metastases are formed beneath the gray/white junctions; i.e., in the area where the size of blood vessels changes and can trap the tumor cells. The BBB and the basement membrane of the brain endothelium protect the brain microenvironment from the majority of the blood-borne components. On the other hand, the cells that create the BBB, including endothelial cells, can express a variety of chemokines and adhesion molecules (Botchkina et al., 1997; Frigerio et al., 1998; Hofman et al., 1998; Zidovetzki et al., 1998) that facilitate adhesion and transendothelial migration of tumor cells. It appears that the delivery of tumor cells via the installed microport may allow studying the specific involvement of brain microvessels and the BBB in the formation and treatment of brain metastases.

In summary, we have developed a new vessel port surgical procedure that allows repeated delivery of exogenous substances and/or cells into the ipsilateral hemisphere of small experimental animals, such as mice. The procedure involves the installation of a microport into the ECA and substance delivery via the CCA and the ICA route. The procedure does not interfere with the CNS function or cerebral blood flow and can be used in a variety of applications that involve the BBB. Other novel aspects of this surgical technique include the ability to perform multiple injections, the study of conscious mice well removed from surgery, and the lack of occlusion of the CCA and ICA, maintaining the carotid flow.

Acknowledgments

Contract grant sponsor: NIH; Contract grant numbers: MH 63022, MH 072567, NS 39254, P42 ES 07380.

REFERENCES

Abbott NJ, Ronnback L, Hansson E. Astrocyte–endothelial interactions at the blood–brain barrier. Nat Rev Neurosci 2006;7:41–53. [PubMed: 16371949]

Andras IE, Pu H, Deli MA, Nath A, Hennig B, Toborek M. HIV-1 Tat protein alters tight junction protein expression and distribution in cultured brain endothelial cells. J Neurosci Res 2003;74:255–265. [PubMed: 14515355]

Avison MJ, Nath A, Berger JR. Understanding pathogenesis and treatment of HIV dementia: a role for magnetic resonance? Trends Neurosci 2002;25:468–473. [PubMed: 12183208]

Avraham HK, Jiang S, Lee TH, Prakash O, Avraham S. HIV-1 Tat-mediated effects on focal adhesion assembly and permeability in brain microvascular endothelial cells. J Immunol 2004;173:6228–6233. [PubMed: 15528360]

Bardelmeijer HA, Ouwehand M, Buckle T, Huisman MT, Schellens JH, Beijnen JH, van Tellingen O. Low systemic exposure of oral docetaxel in mice resulting from extensive first-pass metabolism is boosted by ritonavir. Cancer Res 2002;62:6158–6164. [PubMed: 12414642]

Begley DJ. Delivery of therapeutic agents to the central nervous system: the problems and the possibilities. Pharmacol Ther 2004;104:29–45. [PubMed: 15500907]

Bickel U, Yoshikawa T, Pardridge WM. Delivery of peptides and proteins through the blood–brain barrier. Adv Drug Deliv Rev 2001;46:247–279. [PubMed: 11259843]

Blakeley J. Drug delivery to brain tumors. Curr Neurol Neurosci Rep 2008;8:235–241. [PubMed: 18541119]

Botchkina GI, Meistrell ME 3rd, Botchkina IL, Tracey KJ. Expression of TNF and TNF receptors (p55 and p75) in the rat brain after focal cerebral ischemia. Mol Med 1997;3:765–781. [PubMed: 9407552]

de Boer AG, Gaillard PJ. Drug targeting to the brain. Annu Rev Pharmacol Toxicol 2007;47:323–355. [PubMed: 16961459]

El-Hage N, Wu G, Wang J, Ambati J, Knapp PE, Reed JL, Bruce-Keller AJ, Hauser KF. HIV-1 Tat and opiate-induced changes in astrocytes promote chemotaxis of microglia through the expression of MCP-1 and alternative chemokines. Glia 2006;53:132–146. [PubMed: 16206161]

Frigerio S, Gelati M, Ciusani E, Corsini E, Dufour A, Massa G, Salmaggi A. Immunocompetence of human microvascular brain endothelial cells: cytokine regulation of IL-1beta, MCP-1, IL-10, sICAM-1 and sVCAM-1. J Neurol 1998;245:727–730. [PubMed: 9808241]

Frisella WA, O'Connor LH, Vogler CA, Roberts M, Walkley S, Levy B, Daly TM, Sands MS. Intracranial injection of recombinant adeno-associated virus improves cognitive function in a murine model of mucopolysaccharidosis type VII. Mol Ther 2001;3:351–358. [PubMed: 11273777]

Hayashi K, Pu H, Tian J, Andras IE, Lee YW, Hennig B, Toborek M. HIV-Tat protein induces P-glycoprotein expression in brain microvascular endothelial cells. J Neurochem 2005;93:1231–1241. [PubMed: 15934943]

Hayashi K, Pu H, Andras IE, Eum SY, Yamauchi A, Hennig B, Toborek M. HIV-TAT protein upregulates expression of multidrug resistance protein 1 in the blood–brain barrier. J Cereb Blood Flow Metab 2006;26:1052–1065. [PubMed: 16395283]

Hofman FM, Chen P, Jeyaseelan R, Incardona F, Fisher M, Zidovetzki R. Endothelin-1 induces production of the neutrophil chemotactic factor interleukin-8 by human brain-derived endothelial cells. Blood 1998;92:3064–3072. [PubMed: 9787140]

Huang RQ, Qu YH, Ke WL, Zhu JH, Pei YY, Jiang C. Efficient gene delivery targeted to the brain using a transferrin-conjugated polyethyleneglycol-modified polyamidoamine dendrimer. FASEB J 2007;21:1117–1125. [PubMed: 17218540]

Kim JH, Kim JH, Park JA, Lee SW, Kim WJ, Yu YS, Kim KW. Blood–neural barrier: intercellular communication at glio-vascular interface. J Biochem Mol Biol 2006;39:339–345. [PubMed: 16889675]

Krebs FC, Ross H, McAllister J, Wigdahl B. HIV-1-associated central nervous system dysfunction. Adv Pharmacol 2000;49:315–385. [PubMed: 11013768]

Kumar P, Wu H, McBride JL, Jung KE, Kim MH, Davidson BL, Lee SK, Shankar P, Manjunath N. Transvascular delivery of small interfering RNA to the central nervous system. Nature 2007;448:39–43. [PubMed: 17572664]

Liu R, Martuza RL, Rabkin SD. Intracarotid delivery of oncolytic HSV vector G47Delta to metastatic breast cancer in the brain. Gene Ther 2005;12:647–654. [PubMed: 15647762]

Margalit O, Eisenbach L, Amariglio N, Kaminski N, Harmelin A, Pfeffer R, Shohat M, Rechavi G, Berger R. Overexpression of a set of genes, including WISP-1, common to pulmonary metastases of both mouse D122 Lewis lung carcinoma and B16-F10.9 melanoma cell lines. Br J Cancer 2003;89:314–319. [PubMed: 12865923]

Misra A, Ganesh S, Shahiwala A, Shah SP. Drug delivery to the central nervous system: a review. J Pharm Pharm Sci 2003;6:252–273. [PubMed: 12935438]

Muldoon LL, Soussain C, Jahnke K, Johanson C, Siegal T, Smith QR, Hall WA, Hynynen K, Senter PD, Peereboom DM, Neuwelt EA. Chemotherapy delivery issues in central nervous system malignancy: a reality check. J Clin Oncol 2007;25:2295–2305. [PubMed: 17538176]

Muller FJ, Snyder EY, Loring JF. Gene therapy: can neural stem cells deliver? Nat Rev Neurosci 2006;7:75–84. [PubMed: 16371952]

Neuwelt EA. Mechanisms of disease: the blood–brain barrier. Neurosurgery 2004;54:131–140. [PubMed: 14683550]discussion 141−132

Oh P, Borgstrom P, Witkiewicz H, Li Y, Borgstrom BJ, Chrastina A, Iwata K, Zinn KR, Baldwin R, Testa JE, Schnitzer JE. Live dynamic imaging of caveolae pumping targeted antibody rapidly and specifically across endothelium in the lung. Nat Biotechnol 2007;25:327–337. [PubMed: 17334358]

Pardridge WM. Drug and gene delivery to the brain: the vascular route. Neuron 2002;36:555–558. [PubMed: 12441045]

Pardridge WM. shRNA and siRNA delivery to the brain. Adv Drug Deliv Rev 2007;59:141–152. [PubMed: 17434235]

Patchell RA. The management of brain metastases. Cancer Treat Rev 2003;29:533–540. [PubMed: 14585263]

Persidsky Y, Potula R, Haorah J. Rodent model systems for studies of HIV-1 associated dementia. Neurotox Res 2005;8:91–106. [PubMed: 16260388]

Pignataro G, Studer FE, Wilz A, Simon RP, Boison D. Neuroprotection in ischemic mouse brain induced by stem cell-derived brain implants. J Cereb Blood Flow Metab 2007;27:919–927. [PubMed: 17119544]

Pu H, Tian J, Andras IE, Hayashi K, Flora G, Hennig B, Toborek M. HIV-1 Tat protein-induced alterations of ZO-1 expression are mediated by redox-regulated ERK1/2 activation. J Cereb Blood Flow Metab 2005;25:1325–1335. [PubMed: 15829913]

Puduvalli VK. Brain metastases: biology and the role of the brain microenvironment. Curr Oncol Rep 2001;3:467–475. [PubMed: 11595114]

Reddy GR, Bhojani MS, McConville P, Moody J, Moffat BA, Hall DE, Kim G, Koo YE, Woolliscroft MJ, Sugai JV, Johnson TD, Philbert MA, Kopelman R, Rehemtulla A, Ross BD. Vascular targeted nanoparticles for imaging and treatment of brain tumors. Clin Cancer Res 2006;12:6677–6686. [PubMed: 17121886]

Rhodes RH, Ward JM. AIDS meningoencephalomyelitis. Pathogenesis and changing neuropathologic findings. Pathol Annu 1991;26:247–276. [PubMed: 1861887]

Sebestyen MG, Budker VG, Budker T, Subbotin VM, Zhang G, Monahan SD, Lewis DL, Wong SC, Hagstrom JE, Wolff JA. Mechanism of plasmid delivery by hydrodynamic tail vein injection. I. Hepatocyte uptake of various molecules. J Gene Med 2006;8:852–873. [PubMed: 16724360]

Singer EJ, Syndulko K, Fahy-Chandon B, Schmid P, Conrad A, Tourtellotte WW. Intrathecal IgG synthesis and albumin leakage are increased in subjects with HIV-1 neurologic disease. J Acquir Immune Defic Syndr 1994;7:265–271. [PubMed: 7906304]

Subramanian A, Harris A, Piggott K, Shieff C, Bradford R. Metastasis to and from the central nervous system—the “relatively protected site.”. Lancet Oncol 2002;3:498–507. [PubMed: 12147436]

Sugiyama Y, Kusuhara H, Suzuki H. Kinetic and biochemical analysis of carrier-mediated efflux of drugs through the blood–brain and blood–cerebrospinal fluid barriers: importance in the drug delivery to the brain. J Control Release 1999;62:179–186. [PubMed: 10518649]

Thorne RG, Emory CR, Ala TA, Frey WH 2nd. Quantitative analysis of the olfactory pathway for drug delivery to the brain. Brain Res 1995;692:278–282. [PubMed: 8548316]

Toschi E, Barillari G, Sgadari C, Bacigalupo I, Cereseto A, Carlei D, Palladino C, Zietz C, Leone P, Sturzl M, Butto S, Cafaro A, Monini P, Ensoli B. Activation of matrix-metalloproteinase-2 and membrane-type-1-matrix-metalloproteinase in endothelial cells and induction of vascular permeability in vivo by human immunodeficiency virus-1 Tat protein and basic fibroblast growth factor. Mol Biol Cell 2001;12:2934–2946. [PubMed: 11598182]

Vantyghem SA, Postenka CO, Chambers AF. Estrous cycle influences organ-specific metastasis of B16F10 melanoma cells. Cancer Res 2003;63:4763–4765. [PubMed: 12941790]

Vyas TK, Shahiwala A, Marathe S, Misra A. Intranasal drug delivery for brain targeting. Curr Drug Deliv 2005;2:165–175. [PubMed: 16305417]

Wei L, Erinjeri JP, Rovainen CM, Woolsey TA. Collateral growth and angiogenesis around cortical stroke. Stroke 2001;32:2179–2184. [PubMed: 11546914]

Witt KA, Davis TP. CNS drug delivery: opioid peptides and the blood–brain barrier. AAPS J 2006;8:E76–E88. [PubMed: 16584136]

Wu G, Barth RF, Yang W, Kawabata S, Zhang L, Green-Church K. Targeted delivery of methotrexate to epidermal growth factor receptor-positive brain tumors by means of cetuximab (IMC-C225) dendrimer bioconjugates. Mol Cancer Ther 2006;5:52–59. [PubMed: 16432162]

Zidovetzki R, Wang JL, Chen P, Jeyaseelan R, Hofman F. Human immunodeficiency virus Tat protein induces interleukin 6 mRNA expression in human brain endothelial cells via protein kinase C- and cAMP-dependent protein kinase pathways. AIDS Res Hum Retroviruses 1998;14:825–833. [PubMed: 9671211]

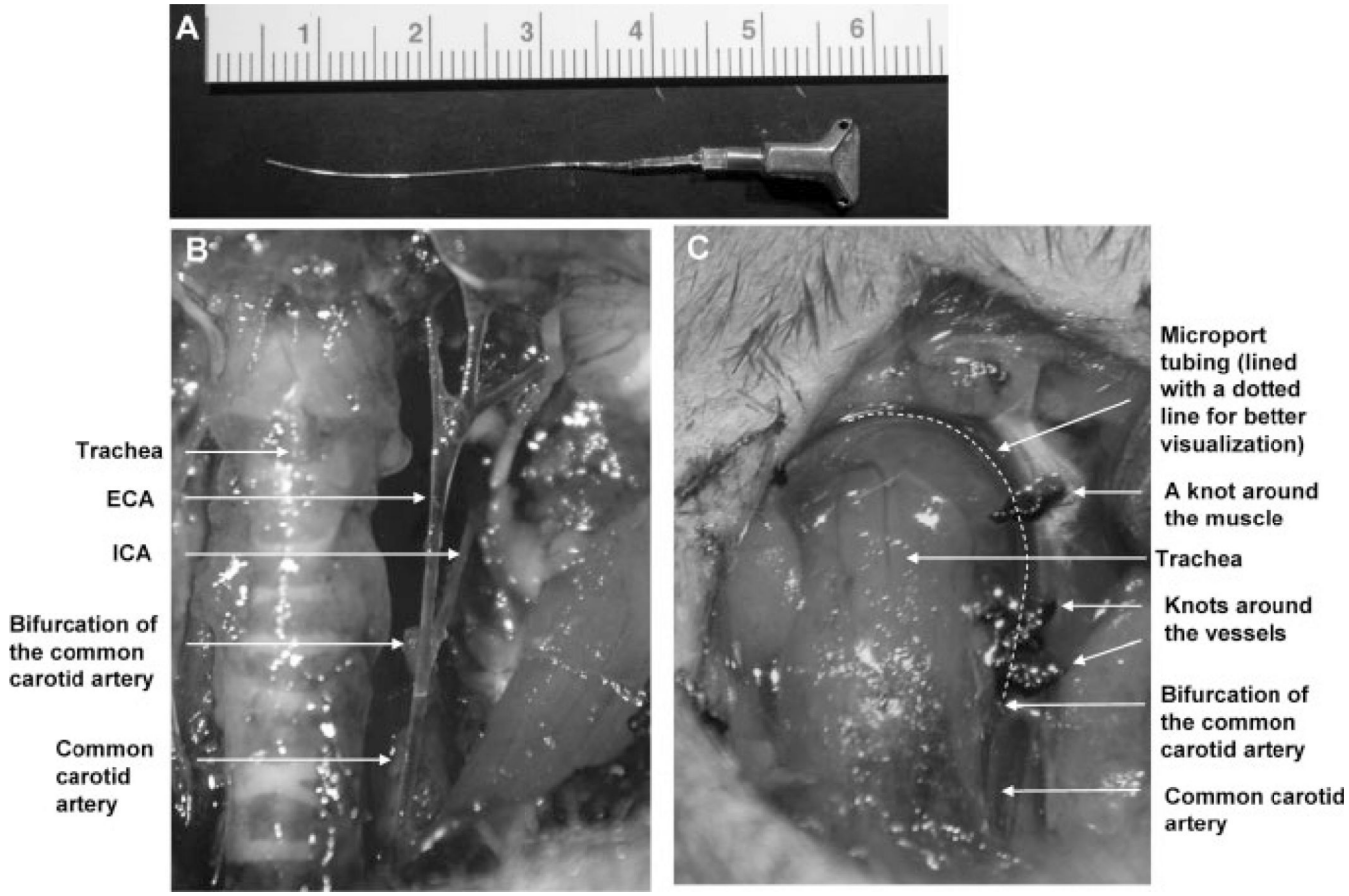

Fig. 1.

Installation of the vessel microport in the external carotid artery (ECA). **A**: Presentation of the vessel port glued to the MRE010 implantation tubing. **B**: Anatomy of the carotid arteries in mice. Common carotid artery (CCA), ECA, and internal carotid artery (ICA) were isolated on the left side of the neck. The cranial thyroid artery and the occipital artery were ligated and cut and are not shown in this figure. **C**: Installation of the vessel microport in the ECA. The microport tubing (outlined with a dotted line for better visualization) was inserted into the ECA and advanced toward the CCA until it reached the bifurcation. The tubing was secured around the ECA and the muscle. The microport was then secured below the skin in the dorsal part of the neck (not shown).

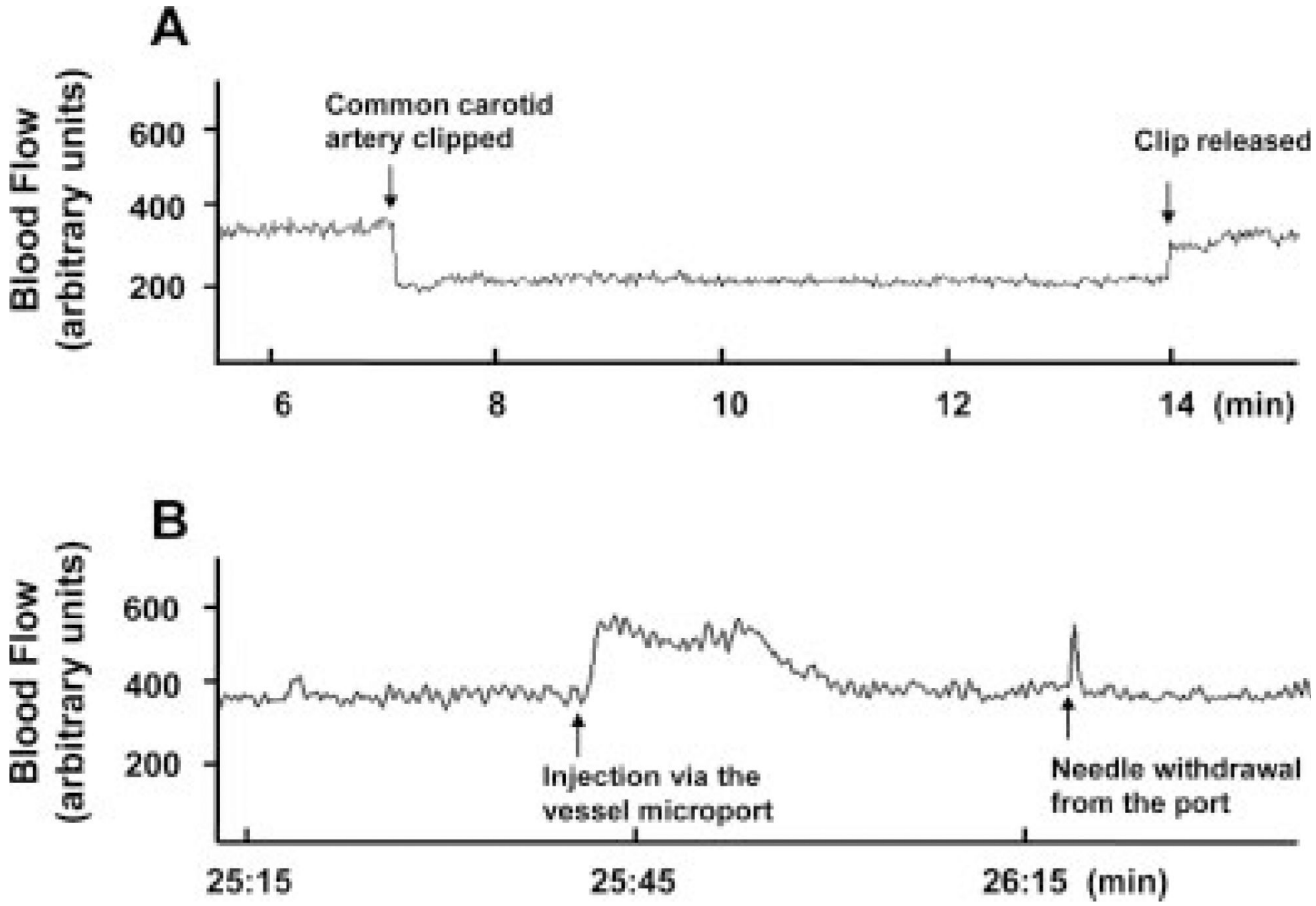

Fig. 2.

Alterations of blood flow during the surgery and substance delivery via the microport. A probe was glued to the mouse skull corresponding to the brain area supplied with blood by the left (i.e., ipsilateral) middle cerebral artery, and the flow in the cortex was monitored by laser Doppler. **A**: A transient decrease in the blood flow as the result of clipping the left common carotid artery (left arrow). The blood flow was restored after the vessel clip was released (right arrow). **B**: Transient alterations of the blood flow following injection of 100 μl PBS through the installed microport.

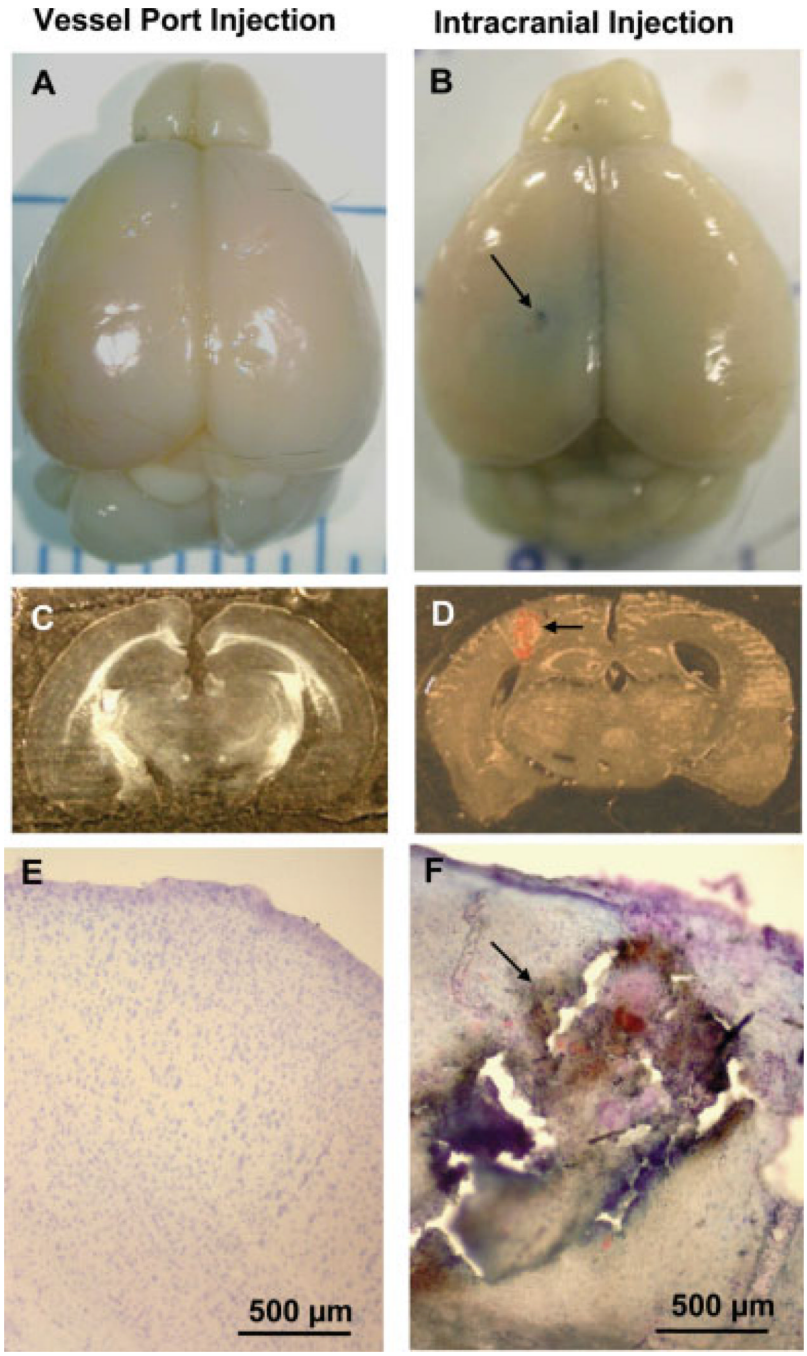

Fig. 3.

Comparison of brain structures in mice that received intracranial vs. microport injections. Mice were injected with 100 μl saline via the vessel port (**left**) or intracranially with 2 μl 2% Evan's blue (**right**). Mice were euthanized and perfused with heparinized saline and euthanatized 24 hr postinjections. Brain sections were stained with cresyl violet. Macroscopic (**A,B**) and microscopic (**C–F**) analyses revealed stab wounds (B,D,F, arrows), tissue damage along the needle mark (D and F, arrows), hemorrhagic changes, and disrupted cortex structure (F, arrow) in mice that received intracranial injections.

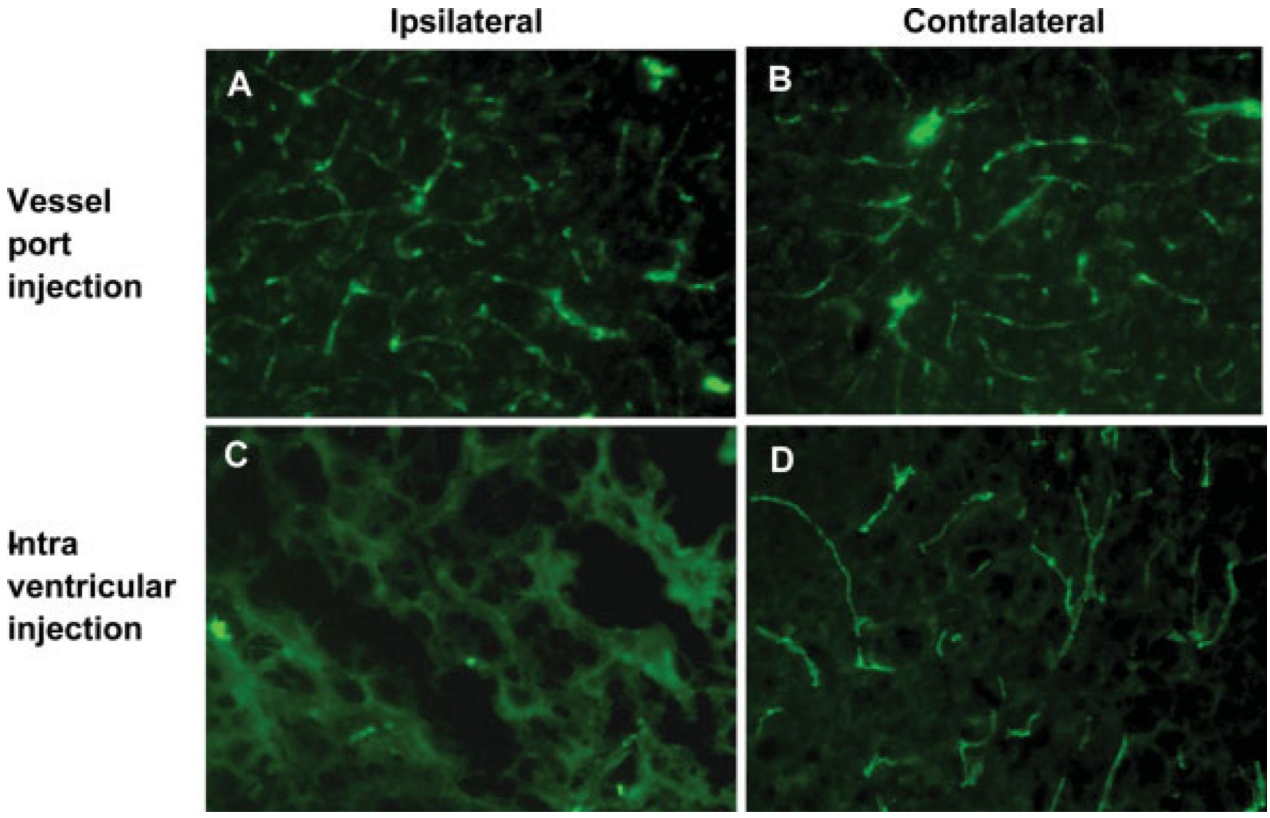

Fig. 4.

Comparison of the integrity of cerebral microvessels in mice that received intracranial vs. microport injections. Injections were performed as described in the legend to Figure 3. Then, the mice were perfused with heparinized saline, followed by 4 ml 2 mg/ml FITC-albumin solution. The integrity of cerebral microvessels was well preserved in mice that received injections via the vessel port (**A,B**) and in the contralateral hemisphere of mice the received intracranial injections (**D**). In contrast, microvessels surrounding the needle puncture were disrupted and permeable, as evidenced by FITC-positive fluorescence in brain parenchyma (**C**).

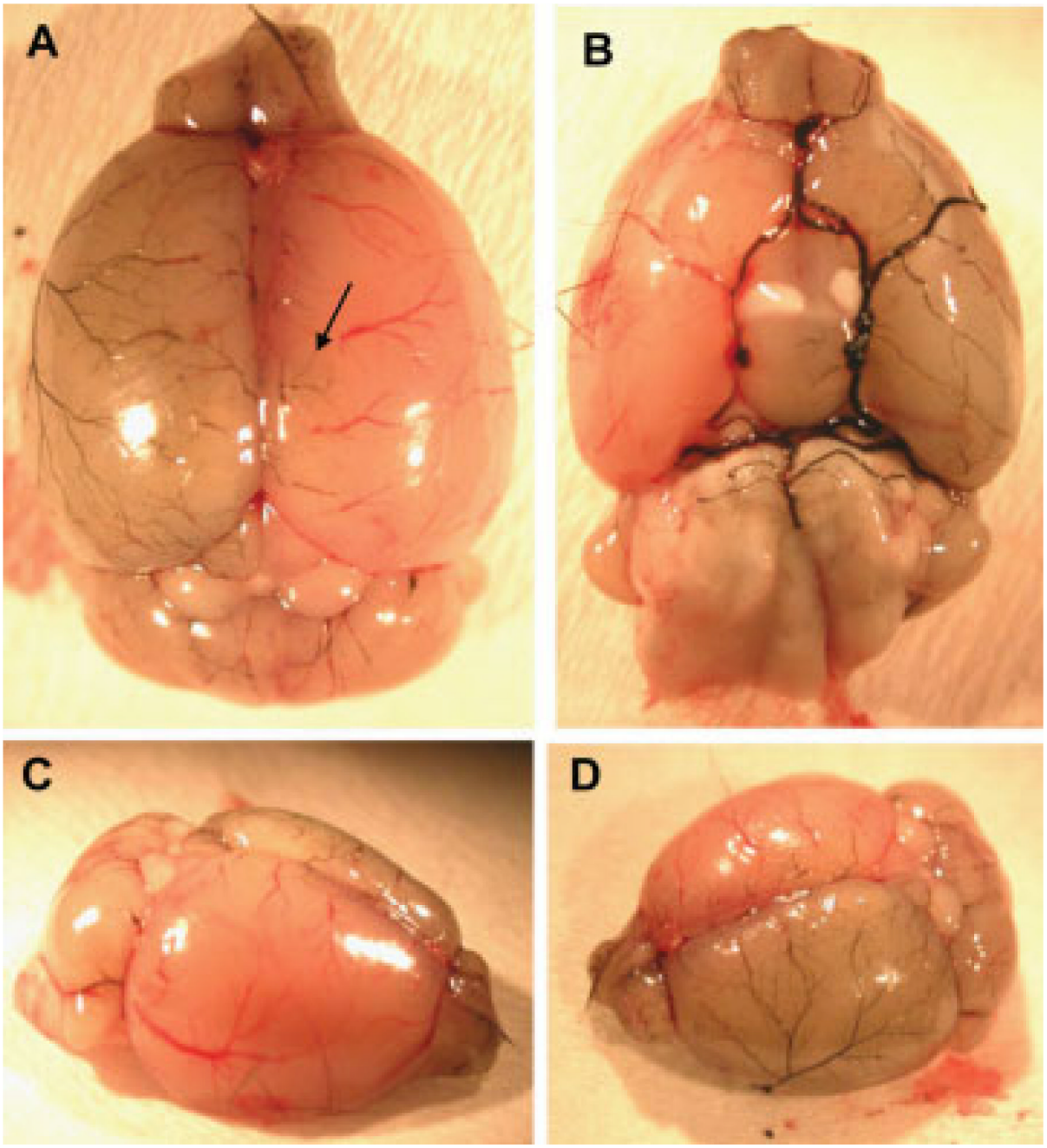

Fig. 5.

Distribution of carbon black in cerebral vessels following injections through the microport. Carbon black (1% solution in 20% gelatin) was injected through the vessel port into anesthetized mice. The brain was harvested and photographed immediately after the injection. Carbon black is visualized primarily in the cerebral vessels of the ipsilateral site. In addition, the staining was positive in small cortical vessels of the contralateral hemisphere (arrow) and in the vessels of the olfactory bulb and the cerebellum at both sites of the brain. **A**: Dorsal view. **B**: Ventral view. **C,D**: Lateral views.

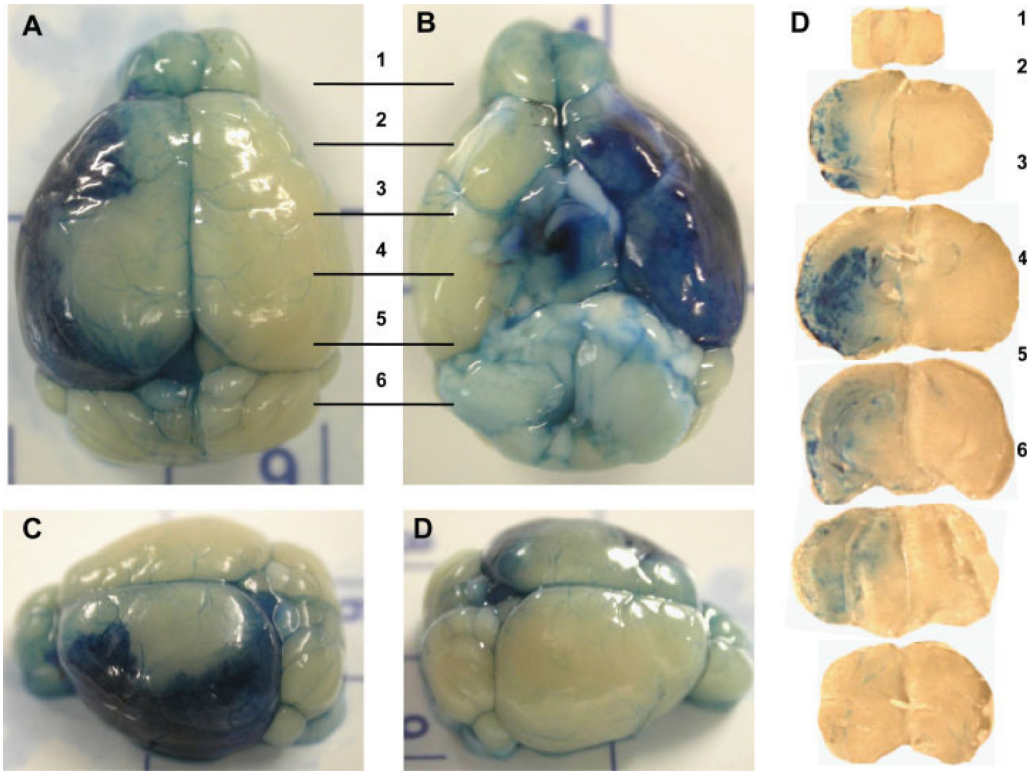

Fig. 6.

Opening of the BBB in the ipsilateral hemisphere following mannitol injection through the microport. Mannitol (200 μl, 2 M solution in PBS) was injected through the vessel port, followed by administration of 200 μl 2% Evan's blue via the tail vein. Mice were perfused with heparinized saline 15 min after Evan's blue administration, and the brains were removed, sliced, and imaged. Evan's blue is localized primarily to the ipsilateral hemisphere. However, less intense staining was also observed in small cortical vessels of the contralateral hemisphere as well as in the cerebellum and olfactory bulb of the contralateral hemisphere. **A**: Dorsal view. **B**: Ventral view. **C,D**: Lateral views. **Right**: Evan's blue staining in the transverse brain sections; the numbers correspond to the areas indicated in A and B.

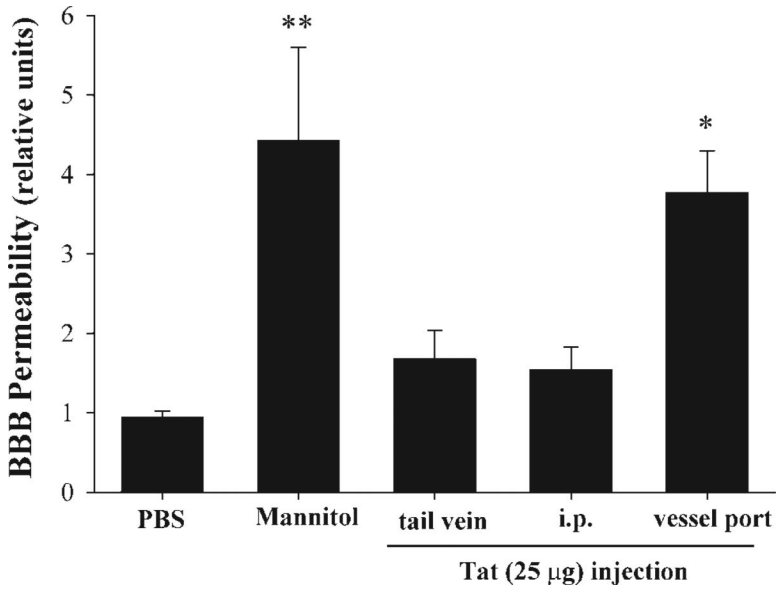

Fig. 7.

HIV-1 Tat-induced disruption of the BBB following injection through the microport. HIV-1 Tat protein (25 μg) was injected through the tail vein, i.p., or via the vessel port. BBB permeability was evaluated in the ipsilateral hemisphere by using the sodium fluorescein method. Analyses were performed 24 hr after Tat injection. Injections with 2 M mannitol or PBS (each at 200 μl via the vessel port) were used as positive or negative controls, respectively. Data are mean ± SEM (n = 5). Data were statistically analyzed by oneway ANOVA, followed by the Newman-Keuls posttest. *$P < 0.05$, **$P < 0.01$ compared with PBS-injected controls.

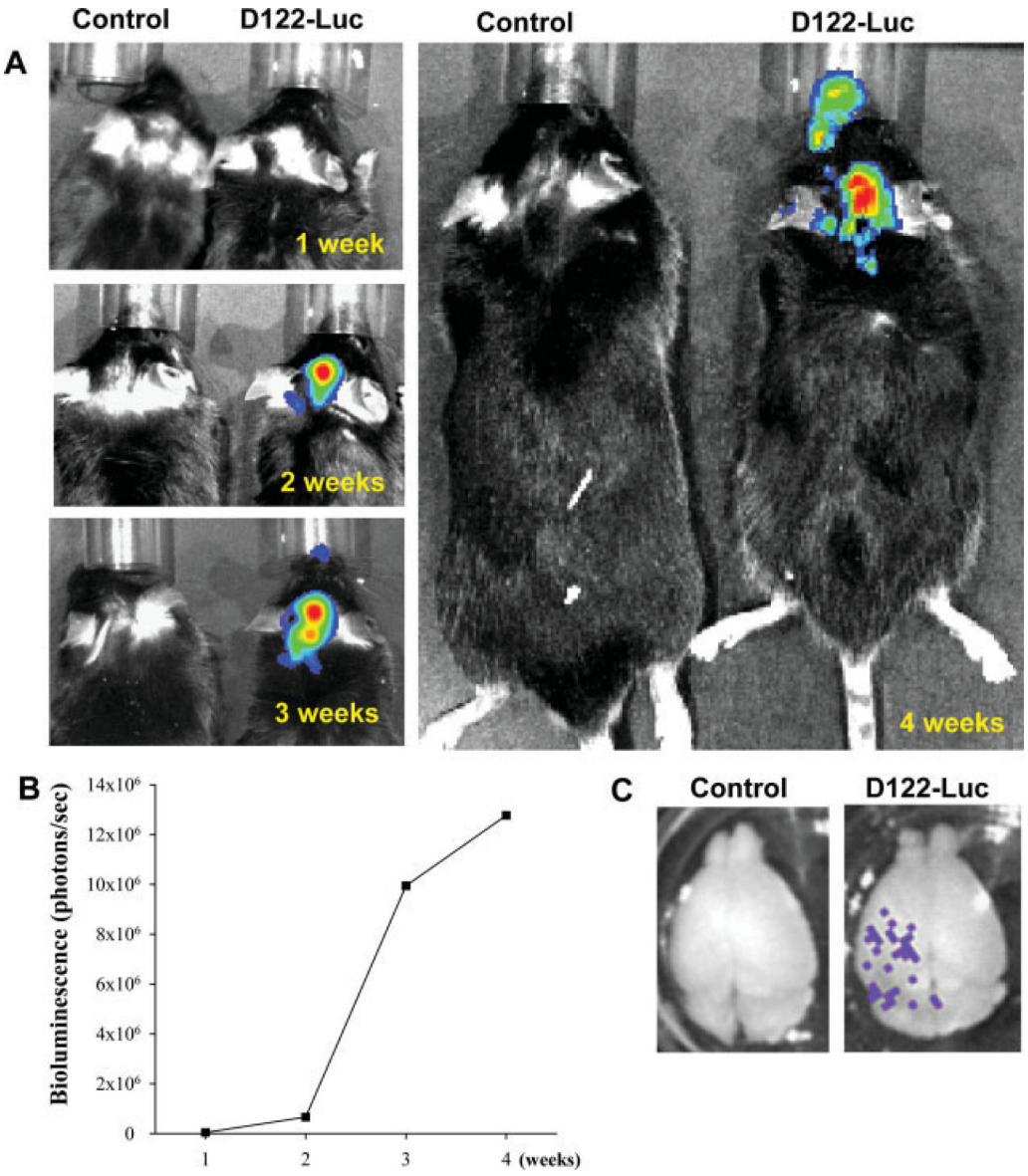

Fig. 8.

Development of brain metastases following tumor cell injection through the microport. To induce brain metastases, 1 million luciferase-labeled D122 cells (D122-Luc) were injected through the vessel port. Bioluminescence signals were recorded by injecting 2 mg luciferin in 100 μl PBS and imaging mice once per week for 4 weeks. Positive signals were recorded only within the heads of mice injected with D122-Luc (**A**) and were steadily increased during the experiment (**B**). The formation of brain metastases was confirmed by recording bioluminescent signal from isolated brains (**C**).